MULTITEMPORAL UNMIXING OF MERIS FR DATA

Raúl Zurita-Milla [a,*], Luis Gómez-Chova[b], Jan G.P.W. Clevers[a], Michael E. Schaepman[a], Gustavo Camps-Valls[b]

[a] Centre for Geo-Information, Wageningen University and Research Centre, Wageningen, The Netherlands
[b] GPDS, Dept. Ingeniería Electrónica, Universidad de Valencia, Dr. Moliner 50, 46100, Burjasot, Spain

Commission VII, WG VII/1

ABSTRACT:

The possibilities of using MERIS full resolution (FR) data to extract sub-pixel land cover composition over The Netherlands are explored in this paper. More precisely, the use of MERIS FR time series is explored in this paper since it should facilitate the discrimination of spectrally similar land cover types because of their seasonal variations. The main steps of the methodology used to extract sub-pixel information can be summarized as follows. First, a set of seven MERIS FR Level 1b images that covered the period February to December 2003 were selected. Second, the images were projected into the Dutch national coordinate system. Special attention was paid to this process in order to account for the orbital differences of each MERIS acquisition. Third, a cloud screening algorithm was applied to all MERIS images. Next, the MERIS level 1b TOA radiances were converted into surface reflectance. After that, the latest version of the Dutch land use database (LGN5) was used to support the selection of the endmembers from the MERIS images. Finally, a constrained linear unmixing algorithm was applied to each of the MERIS scenes and to the multi-temporal dataset. The results were validated both at sub-pixel and per-pixel scales using the LGN5 as a reference. The paper concludes by describing the potential and limitations of the selected approach to extract sub-pixel land cover information over heterogeneous and frequently clouded areas.

1. INTRODUCTION

Obtaining reliable and up-to-date land cover information is essential to better understand the Earth's system. In this respect, the MEdium Resolution Imaging Spectrometer (MERIS) that flies on board the ESA/ENVISAT satellite provides hyperspectral data at unprecedented spatial, spectral and temporal resolutions (Rast and Bezy, 1999). Indeed, MERIS delivers data at 300m (full resolution mode) and at a very high spectral (15 narrow bands) and temporal resolution (revisit time 2-3 days). Because of these characteristics, MERIS has found a number of applications in land remote sensing. For instance, due to its high spectral and temporal resolutions MERIS has been selected to produce a new global land cover map (Arino et al., 2005). However, the use of MERIS for land cover mapping over highly heterogeneous landscapes might not be very appropriate because a number of land cover types will be present in each MERIS pixel. This will lead to the so-called *mixed pixel problem*. In this kind of landscapes, the use of high spatial resolution sensors, like Landsat TM, would be more appropriate. Nevertheless, the temporal and spectral resolutions provided by high spatial resolution sensors are usually not sufficient to accurately map/monitor vegetation dynamics in heterogeneous landscapes. This problem is especially important for areas having persistent cloud coverage throughout the year and/or for areas that have spectrally similar land cover types.

Linear spectral mixture analysis is a relatively straightforward method that can be used to deal with the mixed pixel problem (Settle and Drake, 1993; Ichoku and Karnieli, 1996). In this analysis each pixel is modelled as a linear combination of the pure spectral response of each of the classes that are present in the pixel. Several studies (e.g. Lobell and Asner, 2004) have shown that linear mixture analysis can benefit from a high temporal resolution because, in this case, the classes are not only defined by their spectral signature but also by its evolution over time.

In this paper we are thus concerned with exploring the use of MERIS full resolution (FR) time series to extract sub-pixel land cover information from highly heterogeneous and cloudy areas.

2. STUDY AREA AND DATASETS

2.1 MERIS Full resolution data

A temporal series of MERIS FR level 1b images (geo-located TOA radiances) acquired over The Netherlands in 2003 was selected to illustrate this work. The Netherlands was selected as study area because of the heterogeneity of its landscapes, cloud coverage and the availability of an up-to-date high spatial resolution land use database that can be used to validate the results. The acquisition dates were chosen according to two criteria: (i) to maximize the number of cloud free pixels in each scene and (ii) to get, at least, one image per month so that the phenological cycle is fully captured. Unfortunately, no suitable MERIS FR scene was found for the months of January, March, June, September and November. Therefore, an uneven temporal series of seven images is considered (Table 1).

Table 1. MERIS acquisition dates

18 February	6 August
16 April	15 October
31 May	8 December
14 July	

The MERIS FR images were first projected into the Dutch national system (RD) using the geo-location information provided with the data and a nearest neighbour resampling method. After that, a cloud screening algorithm (Gomez-Chova

---

* Corresponding author. Raul.Zurita-Milla@wur.nl.

et al., 2006) was applied to all the images to identify and mask out cloud contaminated pixels. Then, the TOA radiances were transformed into surface reflectance using an algorithm specifically designed for the MERIS sensor (Guanter et al., 2007). This algorithm is intended for correction of land targets because the low accuracy of aerosol optical thickness retrievals over water. However, in this study, the algorithm was modified to include the first 10km of water from the shoreline in order to obtain surface reflectance over coastal and inland waters, which represent a high percentage of the total area of The Netherlands.

2.2 Reference dataset

The latest version of the Dutch land use database, the LGN5, was used as a reference in this study. This geographical database is based on a multi-temporal classification of high resolution satellite data acquired in 2002 and 2003; several types of ancillary data were also used to produce the land use database – see (Hazeu, 2005) for more details. The LGN5 has a pixel size of 25m and maps 39 classes. The unmixing of all these classes would be unrealistic, since some of the classes are rather small and/or sparsely distributed and/or heavily based on available ancillary data, which mainly describes land uses rather than land covers types. Consequently, the LGN5 was thematically aggregated into the main 12 and 4 land cover types of The Netherlands. The aggregation to 12 classes is meant to offer a detailed distribution of the following classes: grassland, summer crops, winter crops, orchards, deciduous forest, coniferous forest, water, built-up, greenhouses, bare soil (including sand dunes), heathlands, and swamps. The aggregation to 4 classes considers the following main land cover classes: vegetation, bare soil, water and built-up. Despite its simplified legend, the aggregation to 4 classes is of great interest because it can be used as a proxy of fractional vegetation cover and because it might be of help during the inversion of biophysical and biochemical parameters. For example, the presence of sub-pixel water in a pixel might bias the LAI estimate.

3. SPECTRAL UNMIXING

A fully constrained linear spectral unmixing (FCLSU) was applied to each MERIS image (mono-temporal case) as well as to a multitemporal composite (layerstack) of all the MERIS images. The FCLSU (Heinz and Chang, 2001), which guarantees a physical interpretation of the results, can be formalized as follows:

$$p_i = \sum_{c=1}^{c=nc} (f_c \cdot \mu_{ci}) + \varepsilon_i \qquad (1)$$

Subject to:

$$0 \le f_c \le 1 \quad \text{and} \quad \sum_{c=1}^{c=nc} f_c = 1 \qquad (2)$$

where p_i is the pixel value for the band-i, nc represents the number of classes that are being unmixed, f_c is the fraction of class-c present in the pixel, and μ_{ci} is the pure signal of the class-c in the band-i (this signal is commonly known as "class endmember"). Finally, the term ε_i represents the per band residual error.

Notice that the number of dates used in multitemporal unmixing is pixel dependent (each pixel was unmixed with the maximum number of cloud free dates). This means that the quality of the unmixing might also be pixel-dependent and that, if critical (phenological) dates are missing for a number of pixels (areas), the accuracy of the results on those pixels (areas) might be lower.

3.1 Selection of endmembers

A fully automatic class endmember selection method was used in this study. The method only needs the land cover fractions computed for each MERIS date using the LGN5 as a reference and the cloud mask that belongs to each MERIS image. First, the fractions of each land cover class were summed up for all the acquisition dates. Next, these "multitemporal fractions" were used to compute a multitemporal version of the standard purity index, SPI (Zurita-Milla, 2007):

$$SPI = \sqrt{\sum_{c=1}^{c=nc} (f_c - f_{maxclass})^2 \Big/ (nc - 1)} \qquad (3)$$

where f_c represents the multitemporal fraction of class-c in a given pixel and $f_{maxclass}$ is the maximum multitemporal fraction. Therefore, the multitemporal SPI equals one when the pixel has only one class for all the dates under study, and it equals zero when the sum of the fractions is the same for all the classes ($f_c = f_{maxclass} = 1/nc$).

Pure pixels were identified for each date by first applying the corresponding cloud mask to the multitemporal SPI image and then applying a SPI threshold to the remaining (cloud free) pixels. The SPI threshold was adaptively tuned until at least 20 pixels were found for all classes. After that, a neighbourhood constraint is applied to these SPI pure pixels: only the pure pixels surrounded by pure pixels of the same land cover class are selected to compute the endmembers (erosion filter of 3 by 3 pixels). If after applying the neighbourhood constraint a class has less than 5 pixels left, then the constraint is relaxed and all the pixels identified in the previous step are selected as pure pixels to compute the endmember of that class. Finally, the endmembers of each class were created by averaging the pure pixels identified in the previous step.

3.2 Validation datasets

Although the MERIS sensor has a large swath that allows a revisit time of 2-3 days, the ENVISAT platform only repeats orbit every 35 days. This means that each of the MERIS images that were selected for the analysis might have been acquired from a slightly different orbit. This, in turn, implies that each of the MERIS images might have a slightly different observation geometry. Therefore some (sub-pixel) differences in the instantaneous field of view of each "pixel" are to be expected when using images acquired from different orbits.

In order to account for this effect, each MERIS pixel was reprojected into the original LGN5 25m grid so that the "actual land cover fractions" seen by MERIS at each acquisition date could be computed. After this, the sub-pixel land cover fractions were assigned to the corresponding 300 by 300m MERIS pixel. The class having the highest fractional coverage was used to produce a hard land cover classification for each MERIS acquisition date. This processing step allows both a

sub-pixel and a per-pixel validation of the unmixing results for each of the MERIS FR images.

In order to create a validation dataset for the multitemporal results, the LGN5 was spatially aggregated to match the nominal MERIS FR pixel size. A majority filter with a kernel of 12 by 12 LGN5 pixels was used to obtain a land cover classification map at 300m. During this spatial aggregation, the fractions of the different land cover types present in each 300 by 300m pixel were recorded.

3.3 Accuracy assessment

The fractional maps computed in the previous section were used as ground truth for the validation of the monotemporal and multitemporal unmixing. Assuming that the unmixed fractions are correctly positioned within each pixel, a kind of overall sub-pixel accuracy (OSA) can be computed as follows:

$$OSA = \sum_{c=1}^{c=nc} d_c \bigg/ \sum_{c=1}^{c=nc} f_c = \sum_{c=1}^{c=nc} d_c$$

$$d_c = \min\left\{ f_c^{LGN5}, f_c \right\}$$

(4)

where d_c are the correctly classified abundances for each pixel. These abundances can be computed as the minimum of f_c^{LGN5} and f_c, which respectively are the LGN-based and the unmixed abundances. Notice that the sum of f_c for all classes adds to unity (Eq. 2).

After the sub-pixel accuracy assessment, the unmixed fractions were used to produce land cover classification maps for each date. The class having the maximum fractional coverage was used to label each pixel. Subsequently, a classical classification accuracy assessment was done by comparing these images with the land cover maps that were computed for each date. Similarly, the hard classified multitemporal image was validated using the aggregated LGN5 as a reference. The confusion matrix and the kappa index were used for the per-pixel accuracy assessment.

4. RESULTS AND DISCUSSION

4.1 MERIS pre-processing

A visual inspection of the reprojected MERIS images did not show any major shift between them (besides the expected differences due to different acquisition orbits). Images also overlapped quite well the reference dataset. This can be considered as a preliminary quality proof of the ground control points provided with the images. Although a quantitative assessment of the geolocation accuracy might have been more appropriate, here we decided to keep it simple in order to also test the operability of the unmixing of MERIS FR time series. Therefore, in this study, the pre-processing steps were reduced as much as possible.

With respect to the cloud screening method, all the clouds and cloud borders were masked out. The validation of the cloud mask revealed that a small amount of pixels belonging to the classes greenhouses (sun glint on glass roofs) and bare soil (sand dunes) were identified as clouds because these classes have similar reflectance behaviour as clouds. However, the classes that were misclassified represent less than 0.5% of The Netherlands and, therefore, they are not statistically representative in the clustering process used by the cloud screening algorithm.
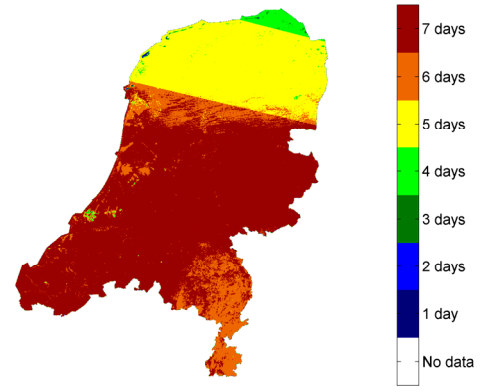

Figure 1. Total number of usable dates

Figure 1 shows the number of usable dates for each MERIS FR pixel. It should be noted that the northern and south-eastern parts of the Netherlands have less usable pixels than the rest of the country. This is not only because of the cloud coverage but also because some of the MERIS FR images did not cover the whole of The Netherlands.
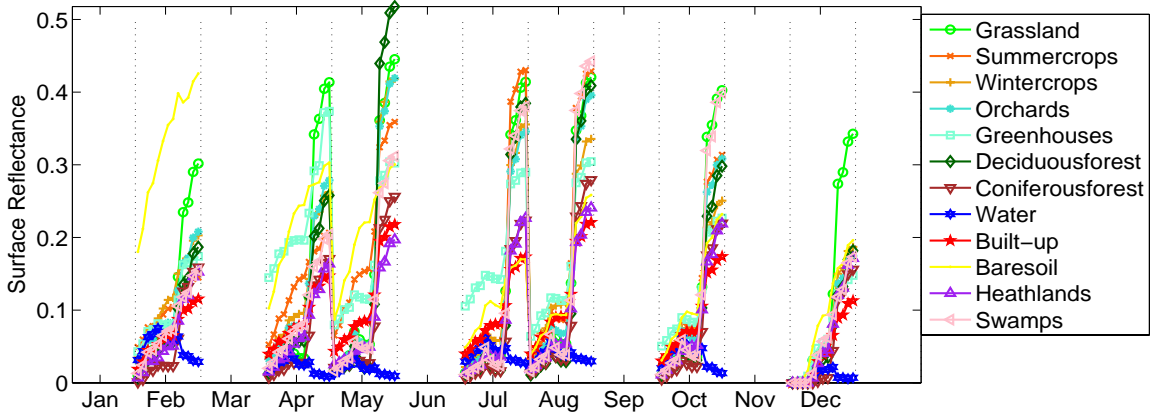

Figure 2. Spectral signature of the endmembers extracted from the MERIS FR time series.

Table 2. Summary of the accuracy assessment for the 12 classes case

Date	18-2-2003	16-4-2003	31-5-2003	14-7-2003	6-8-2003	15-10-2003	8-12-2003	Multitemp
mean OSA	43.54	52.70	42.35	45.46	36.88	41.56	44.78	52.72
Kappa	0.33	0.44	0.33	0.36	0.27	0.30	0.32	0.45
OA	44.29	54.17	43.88	46.06	35.29	41.87	45.68	55.17

Table 3. Summary of the accuracy assessment for the 4 classes case

Date	18-2-2003	16-4-2003	31-5-2003	14-7-2003	6-8-2003	15-10-2003	8-12-2003	Multitemp
mean OSA	77.20	82.84	78.21	83.07	80.01	74.52	74.28	82.51
Kappa	0.52	0.73	0.60	0.69	0.58	0.50	0.50	0.71
OA	80.83	88.27	83.09	87.28	82.54	76.66	77.56	87.81

Table 4. User's and producer's accuracies (UA and PA, respectively) for the 12 classes case

Class	Grassland	Summer Crops	Winter Crops	Orchards	Greenhouses	Deciduous. Forest
UA	70.96	58.40	17.59	4.19	16.27	13.40
PA	72.90	26.29	18.58	0.97	68.66	35.79
Class	Coniferous Forest	Water	Built-up	Bare soil	Heathlands	Swamps
UA	50.09	86.95	71.67	10.79	13.72	5.05
PA	71.78	88.70	41.45	37.17	31.88	15.17

Table 5. User's and producer's accuracies (UA and PA, respectively) for the 4 classes case

Class	Vegetation	Bare soil	Water	Built-up
UA	87.58	36.65	92.55	78.42
PA	98.05	24.71	84.79	25.59

4.2 Endmembers

Most of the endmembers were computed as average of the pixels selected using the initial SPI threshold of 0.95. Nevertheless, for some small classes, the SPI threshold was reduced in order to get, at least, 20 pixels for those classes.
For instance, the SPI threshold had to be reduced to 0.87 to extract 20 "pure pixels" of the greenhouse class on cloudy dates (31st May and 6th August). For the small and sparse classes the neighbourhood constraint was, in general, not applied because very few clusters of 3 by 3 pure pixels can be found.
Figure 2 shows the spectral signature of the endmembers selected in this study. Grassland presents the highest NIR reflectance all year around. During the months of May, July and August the endmember of deciduous forest also shows high reflectance (high greening of vegetation). The rest of the vegetated classes appear to have a very similar spectral signature. Therefore, high confusion is expected among most of the vegetated classes.

4.3 Unmixing

A fully constrained linear spectral unmixing was applied to each of the seven MERIS images and to the multitemporal time series using the 12 endmembers depicted in figure 2. The fractions for the 4 classes case were computed by aggregating all the fractions of vegetated classes into a single vegetation class and by grouping the fractions of greenhouses and built-up into a single built-up class. The unmixed fractions were then compared with the reference fractions that were generated according to the viewing geometry of each date (see section 2.3). The overall sub-pixel accuracy (OSA; Eq. 4) was used to do this comparison. As an example, figure 3 illustrates the OSA for the multitemporal unmixing of 12 and 4 classes. In general, homogeneous areas tend to agree well with the reference dataset

and, as expected, the 4 classes case offers better OSA values because the spectral confusion among vegetated classes is now removed. However, in the case of 12 classes, low agreements are found in the north and south eastern part of the country. These areas do not only have more heterogeneous pixels than the rest of the country but were also unmixed using fewer dates. Subsequently, the unmixed fractions were transformed into a hard classification map and the overall classification accuracy (OA) and the kappa statistic were computed by comparing these maps with the reference land cover maps.
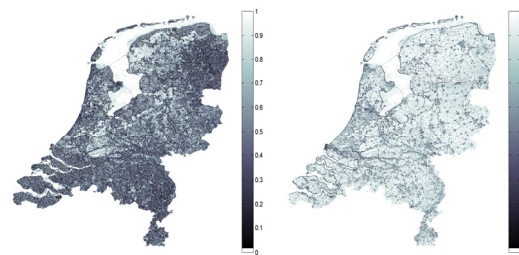

Figure 3. Overall sub-pixel accuracies (OSA) for the multitemporal unmixing of 12 (left) and 4 (right) classes.

Tables 2 and 3 summarise the results of the sub-pixel and per-pixel classification accuracy assessment for the 12 and 4 classes cases. Three main conclusions can be drawn from these tables. (i) Classification results for the 4 classes case are much higher than the results obtained for 12 classes. This is mainly because the vegetated classes are spectrally very similar. (ii) The multitemporal approach yielded the highest classification results, since adding the temporal evolution (phenology) simplifies the discrimination of spectrally similar land cover types. Nevertheless, the difference between the classification results of the best monotemporal image (April) and the
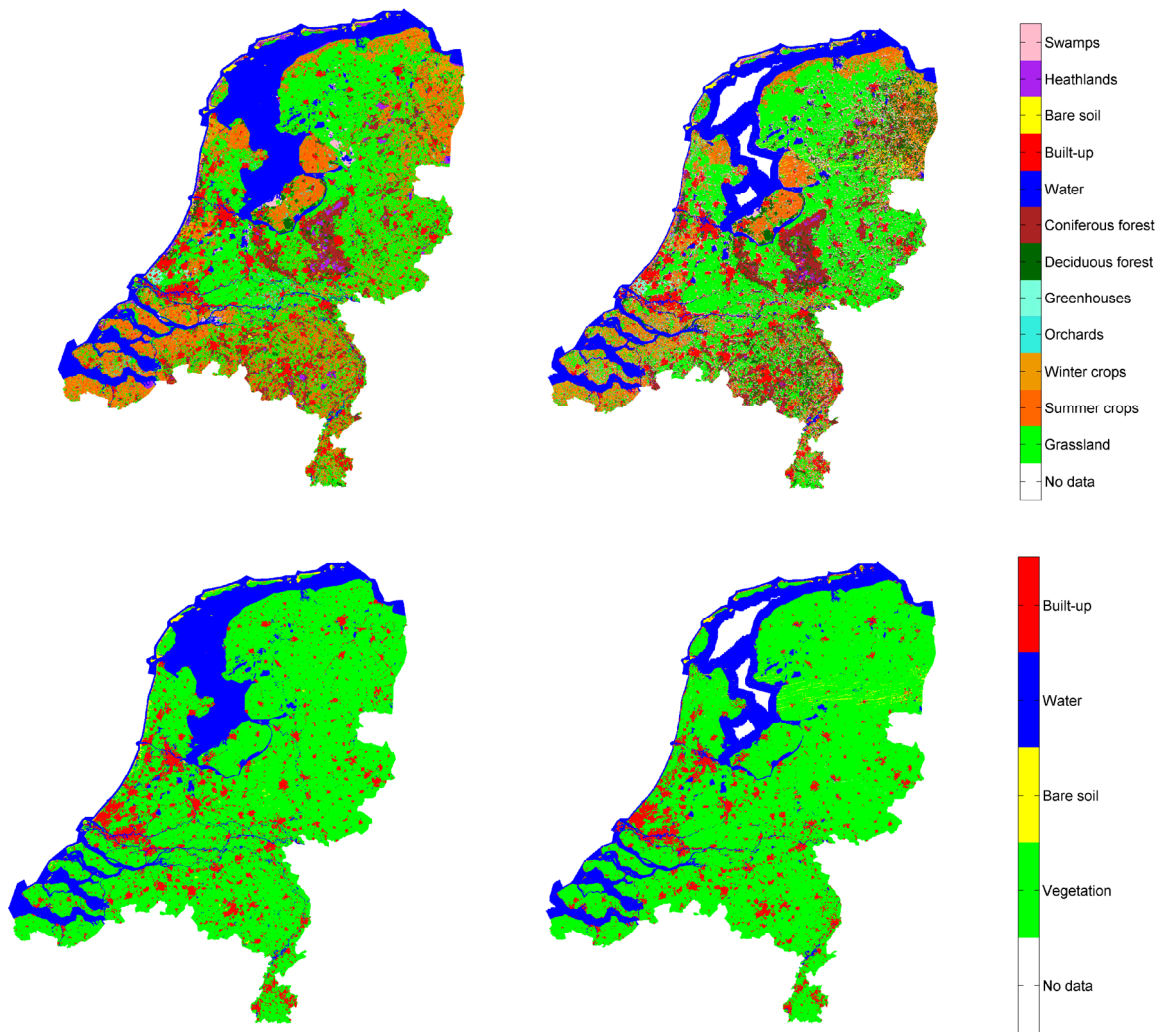
Figure 4. Reference dataset (left) and Multitemporal hard classified images (right) for 12 (top row) and 4 (bottom row) classes.

multitemporal approach is not very large. This indicates that the selection of the dates for the unmixing is critical (e.g. in spring most of the vegetated classes appear to have a large separability). (iii) The OSA and the OA values are in the same order of magnitude. However, the OSA refers to the sub-pixel abundances and therefore it inherently contains more information than the OA computed from the hard classified images.

Figure 4 shows the reference datasets and the hard classification results that were obtained for the multitemporal 12 and 4 classes cases. Notice that the gap in the inland waters of the north of Netherlands is caused by the atmospheric correction (recall that only the first 10 km of coastal water were atmospherically corrected).

Finally, Tables 4 and 5 show the user's and producer's accuracies for the multitemporal case. For the 12 classes unmixing, the classes orchards, swamps and winter crops present the three poorest producer's and user's accuracies followed by the classes heathlands, bare soil and deciduous forest. This suggests that a further simplification of the 12 classes cases is needed. With respect to the 4 classes case only the bare soil class appears to have poor user's and producer's accuracies. This could be due to fact that the class bare soil is rather small (it mainly comprises sand dunes in coastal areas).

5. CONCLUSIONS

This study has shown that the use of MERIS FR data has a great potential to extract sub-pixel land cover composition over heterogeneous and frequently clouded areas. The multitemporal unmixing of MERIS FR data yielded sub-pixel and per-pixel overall accuracies that were very similar to the ones obtained for the best monotemporal image. This indicates that the selection of dates used for the unmixing is critical. Vegetation phenophases and the spectral separability of the endmembers should be further studied in order to optimize the best combination of dates and classes to be unmixed. Nevertheless, we should keep in mind that all the unmixing results have been validated using a static dataset produced using a combination of high resolution satellite data from 2002 and 2003 and several sources of ancillary data. Thus, validation results might be slightly affected by the period in which the reference dataset was produced.

The overall classification accuracy (OA) for the multitemporal 12 classes case was moderately good (around 55%) while the aggregated 4 classes case yielded better OA (around 88%). Furthermore, the overall sub-pixel accuracies (OSA values) were in the same order of magnitude as the overall classification accuracy. Therefore, we are confident that the extracted sub-pixel information might be of great utility in remote sensing monitoring activities, such as land cover change detection or retrieval of biophysical parameters from MERIS

FR data. Additional work will be devoted to the use of the 4 classes case as a proxy of fractional vegetation cover.

REFERENCES

Arino, O., Trebossen, H., Achard, F., Leroy, M., Brockman, C., Defourny, P., Witt, R., Latham, J., Schmullius, C., Plummer, S., Laur, H., Goryl, P. and Houghton, N., 2005. The globcover initiative. European Space Agency, (Special Publication) ESA SP 597, pp 171-175.

Gomez-Chova, L., Camps-Valls, G., Amoros-Lopez, J., Guanter, L., Alonso, L., Calpe, J. and Moreno, J., 2006, New Cloud Detection Algorithm for Multispectral and Hyperspectral Images: Application to ENVISAT / MERIS and PROBA / CHRIS Sensors. IEEE International Geoscience and Remote Sensing Symposium. Denver, Colorado, July 31-August 4, 2006.

Gomez-Chova, L., Camps-Valls, G., Amoros-Lopez, J., Martín, J.D., Calpe, J., Alonso, L., Guanter, L., Fortea, J. C. and Moreno, J., 2006. Cloud detection for MERIS multispectral images. Proceedings of the MERIS (A)ATSR Workshop. ESA Publications Division, ESA SP-597.

Guanter, L., González-Sampedro, M. C. and Moreno, J., 2007. A method for the atmospheric correction of ENVISAT/MERIS data over land targets. *International Journal of Remote Sensing*, vol. 28(3), pp. 709–728.

Hazeu, G., 2005. The Dutch Land Use Database LGN. http://www.lgn.nl/ (accessed 19 Feb. 2007)

Heinz, D. and Chang, C.-I., 2001, Fully constrained least squares linear mixture analysis for material quantification in hyperspectral imagery, *IEEE Transactions on Geoscience and Remote Sensing*, vol. 39(3), pp. 529–545.

Ichoku, C. and Karnieli, A., 1996. A review of mixture modelling techniques for sub-pixel land cover estimation. *Remote Sensing Reviews*, 13, pp. 161-186.

Lobell, D.B. and Asner, G.P., 2004. Cropland distribution from temporal unmixing of MODIS data. *Remote Sensing of Environment*, 93, pp. 412-422.

Rast, M, and Bezy, J.L., 1999. The ESA Medium Resolution Imaging Spectrometer MERIS a review of the instrument and its mission, *International Journal of Remote Sensing*, 20(9), pp. 1681 – 1702.

Settle, J.J. and Drake, N.A., 1993. Linear mixing and the estimation of ground cover proportions. *International Journal of Remote Sensing* 14(6), pp. 1159-1177.

Zurita-Milla R., Clevers, J. G. P. W., Schaepman, M. E. and Kneubuchler, M., 2007. Effects of MERIS L1b radiometric calibration on regional land cover mapping and land products. *International Journal of Remote Sensing* 28(3), pp. 653-673